CHAPTER 3

EXPERIMENTAL PROCEDURES

This chapter describes all the experimental procedures employed in this work. It is appropriate to discuss the various experimental aspects of powder preparation, ceramic fabrication, and characterization. Phase formation characterization has been carried out using X-ray diffraction. Microstructural development has been examined via electron microscopy techniques (i.e. SEM and TEM) in conjunction with energy dispersive X-ray (EDX) analysis. Dielectric measurement technique has been used to determine the properties of the materials.

3.1 Sample Preparation

All powders and ceramics were produced using various preparation methods as described here.

3.1.1 Powder Preparation

In this work, all powders have been prepared by a mixed oxide technique. All commercially available starting compounds which were used for the preparation of the compositions in this study are listed in Table 3.1, along with the suppliers, formula weights and purities. These oxides were re-checked by X-ray diffraction technique in order to determine their phase compositions and impurities.

Table 3.1 Specifications of the starting materials used in this study.

Powder	Source	Formula weight	Purity(%)
PbO	Fluka*	223.19	> 98
ZrO_2	Riedel-de Haën**	123.22	> 99
TiO_2	Riedel-de Haën**	79.90	> 99
MgO	Fluka*	40.31	> 98
Nb_2O_5	Aldrich***	265.81	99.9

Note: * Fluka Chemical GmbH, Switzerland

** RdH Laborchemikalin GmbH & Co. KG, Germany

*** Aldrich Chemical Company Inc., USA.

Both of the PZT and PMN powders were synthesized by using the B-site precursor method via zirconium titanate ($ZrTiO_4$ or ZT) and magnesium niobate ($MgNb_2O_6$ or MN) precursors, respectively, prior to mixing and reacting with PbO in the second step of calcination at an elevated temperature. During the process, a two-step calcination technique was applied as their associated chemical reactions can be expressed:

For the preparation of PZT powders;

Step 1 $ZrO_2 + TiO_2 \longrightarrow ZrTiO_4$ (3.1)

Step 2 $2PbO + ZrTiO_4 \longrightarrow 2Pb(Zr_{0.5}Ti_{0.5})O_3$ (3.2)

For the preparation of PMN powders;

Step 1 $MgO + Nb_2O_5 \longrightarrow MgNb_2O_6$ (3.3)

Step 2 $PbO + (1/3)\ MgNb_2O_6 \longrightarrow Pb(Mg_{1/3}Nb_{2/3})O_3$ (3.4)

Mixing and calcination processes schematically illustrated in Fig. 3.1 were employed as a routine processing procedure for all powder compositions in this work. In the mixing process, the calculated relevant proportions of constituents were weighted, suspended in ethanol and intimately mixed in a ball-mill, for 24 h with zirconia media. Drying was carried out for 2 h, prior to sieving through about 30 μm mesh. The dried powder was then ground, sieved and calcined in closed alumina crucibles. Conditions for optimizing the calcination were carefully determined.

The B-site precursor powders obtained from the optimum calcination condition were then mixed with PbO, seperately. Mixing process for the preparation of PZT and PMN powders were performed according to the MCP method (see Fig. 3.1). Then, mixed powder was heat treated at various temperatures, dwell times and heating/cooling rates. Powders were analysed by XRD to identify the optimum calcination condition for the formation of perovskite phase (Fig. 3.2).

Each composition in *x*PZT-(1-*x*)PMN system was prepared by weighing required proportions of PMN and PZT components. The mixing process described in Fig. 3.3 was followed.

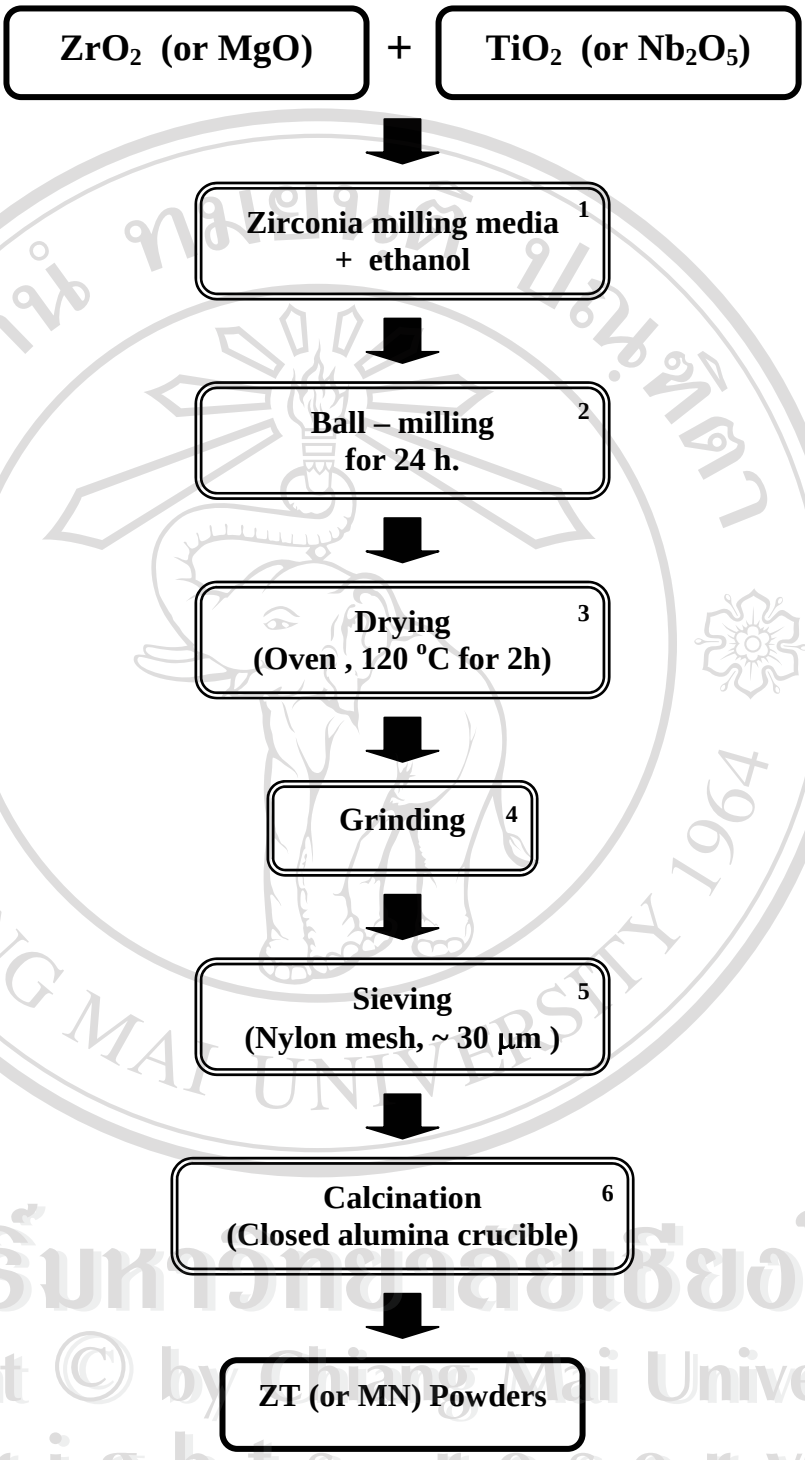

Fig. 3.1 Mixing and calcination processes or MCP (step 1-6) for B-site precursor preparation.

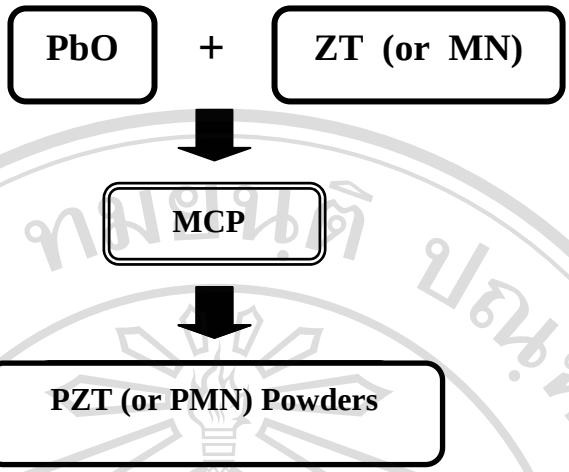

Fig. 3.2 Flow chart for the preparation of PZT and PMN powders.

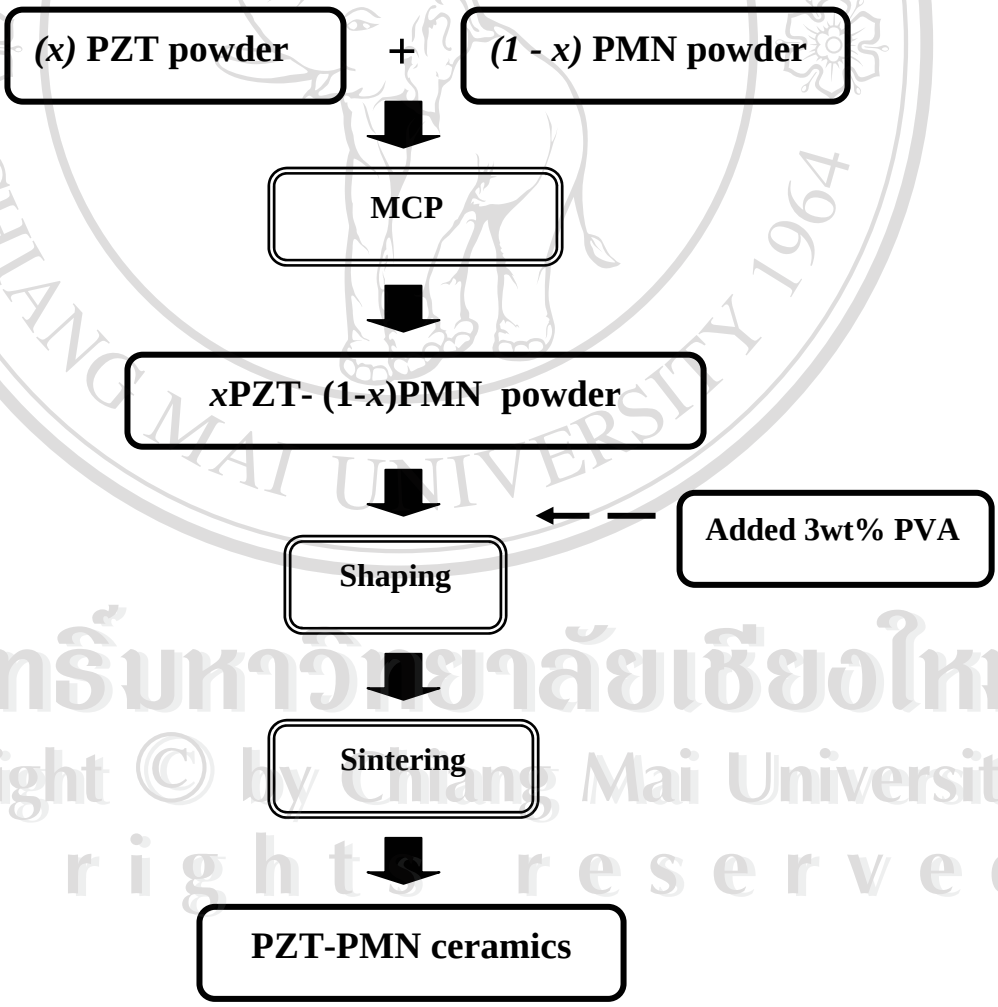

Fig. 3.3 Flow chart for the fabrication of PZT-PMN ceramics.

3.1.2 Ceramic Fabrication

In this work, all ceramic compositions have been fabricated by uniaxial pressing the powder (~ 2 g) of each composition into a green pellet of diameter 10 mm and sintered at various conditions in a high temperature furnace. To aid pressing and green densification, 3 wt% polyvinyl alcohol (PVA) binder was added into the calcined powders prior to pressing. After the binder was burnt out at 500 ^{o}C for 2 h, the sample was placed on the $PbZrO_3$ powder-bed inside the alumina powder, in order to reduce loss of volatile components. This assembly is arranged inside closed alumina crucible, as shown in Fig. 3.4, before insertion into a high temperature furnance.

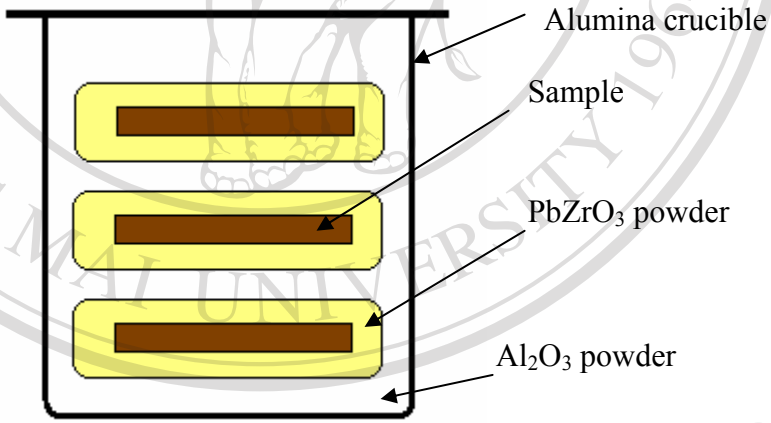

Fig. 3.4 Sample arrangement for the sintering process.

3.2 Sample Characterization

All powders and ceramics were characterized using different tools as described below.

3.2.1 Differential Thermal Analysis (DTA) and Thermogravimetric Analysis (TGA)

Thermal decomposition and weight loss behaviour of the uncalcined powders was analysed by Differential Thermal Analysis (DTA) and thermogravimetric analysis (TGA). In this experiment, Stanton Redcroft DTA 673-4 module (Fig. 3.5) and Perkin Elmer TGA7 (Fig. 3.6) were employed with platinum crucibles, reference powder of Al_2O_3 and a heating rate of 10 ^oC/min. The decomposition temperature and weight loss were recorded when the samples were heated from room temperature to 1300 ^oC.

Fig. 3.5 Differential thermal analysis (Stanton Redcroft DTA 673-4).

Fig. 3.6 Thermogravimetric analysis (Perkin Elmer TGA7)

3.2.2 X-ray Diffraction (XRD)

Room temperature X-ray diffraction studies were carried out with the Philips (Model X-pert) automatic powder diffraction system (Fig. 3.7). The diffractometer was operated at 40 kV with 20 mA current. Monochromatic Cuk_{α} radiation of wavelength 1.540562 Å was used throughout. For all measurements, a scan step mode was used with a step size of 0.02 ^{o} per second. Each sample was scanned for a 2θ-range from 10-60 ^{o}. A computer program (X-pert Plus Software and CaRIne software version 3.1) was used to determine lattice parameters of the samples upon the X-ray powder diffraction database of ICDD* version 2000.

* International Centre for Diffraction Data (ICDD), Newtown Square, PA, USA

Fig. 3.7 X-ray diffractometer (Philips Model X-pert).

The amount of the major phase present in each sample may, in principle, was estimated using the following equation as suggested in the literature[19] on the basis of relative intensities of the major X-ray reflections for the major and the minor phases:

$$\text{Perovskite phase (wt \%)} = \left(\frac{I_{major}}{I_{major} + I_{minor}} \right) \times 100 \qquad (3.5)$$

where I_{major} and I_{minor} refer to the intensity of the majority phase and minority phase, respectively.

3.2.3 Densification Measurement

The densities of all samples were determined using the Archimedes' method. The sample is first weighed dry (W_1), then weighed again after fluid impregnation (W_2), and finally weighed while being immersed in water (W_3). All weights are in

grams. Generally, a very thin brass wire is used to suspend the sample in the water and its weight W_w must be measured in water, too. Then the density (ρ) can be calculated from the following equation[80]:

$$\rho = \frac{W_1 \rho_w}{W_2 - (W_3 - W_w)} \quad (3.6)$$

where ρ_w is the density of water (in g/cm^3), which is slightly temperature dependent,

$$\rho_w = 1.0017 - 0.0002315T \quad (3.7)$$

when *T* is the temperature of water (in degree Celsius).

The fired shrinkages (and weight loss) of all sintered samples were measured from the percentage diameter (and weight) change with respect to the original diameter (l_o) (and weight, w_o) before sintering.

$$\text{Shrinkage (\%)} = (\Delta l / l_o) \times 100 \quad (3.8)$$

$$\text{Weight loss (\%)} = (\Delta w / w_o) \times 100 \quad (3.9)$$

3.2.4 Scanning Electron Microscopy (SEM)

In this work, A JEOL JSM-840A and Camscan Series II (Cambridge, England) as shown in Fig. 3.8 were used to determine the morphology of the powders, the as-fired and fracture surface of the ceramics. The powders were dispersed in an ethanol using ultrasonic cleaner, and then coated with gold sputtering. As-sintered surface and fracture surface of the ceramics were cleaned by ultrasonic cleaner and coated with carbon. During image acquisition, both backscattered and secondary

electron modes were used with an accelerating voltage of 20 kV. Chemical composition of the selected area was quantified by using an energy dispersive X-ray spectrometry (EDX). The range of grain size and average grain size were determined by applying the linear interception method to the SEM micrograph.

Fig. 3.8 Scanning electron microscope (SEM, Camscan II).

3.2.5 Transmission Electron Microscope (TEM)

PZT and PMN samples for TEM were ground parallel to ~ 25 μm thickness on glass slides using 1200 grit SiC paper. A 3 mm-diameter Cu support ring with a millimeter hole (Agar Scientific Ltd., Essex, England) was glued onto the ground ceramic using epoxy resin. After cleaning with acetone, samples were ion thinned using a Gatan dual ion mill (Model 600, Gatan Inc., Pleasanton, California, USA), operating at an accelerating voltage of 6 kV, a beam current of 0.3 mA per gun, and milling incidence angles of 10-15^{o}. Specimens were coated with carbon (Emitch K950

carbon coater, Pfeiffer Vacuum, Germany) before TEM examination. TEM studies were done on Tecnai 20 (Philips, Holland, operating at 200 kV), as shown in Fig. 3.9.

Fig. 3.9 Transmission electron microscope (TEM, Philips Tecnai 20).

TEM specimens were tilted to a two-beam condition using the double-tilt specimen holder. The two-beam condition is an orientation at which only one set of planes is strongly diffracting. Bright-field (BF) imaging was then achieved by using an objective aperture to cover only the transmitted beam. Electron diffraction patterns were obtained using the selected-area (SA) diffraction technique. To record the SA diffraction, a SA aperture of an appropriate diameter was inserted and the objective aperture was removed. By selecting the right camera length, adjusting the intensity of illumination to a suitable level and focusing, the diffraction pattern was obtained.

3.2.6 Dielectric Measurement

Disc shaped samples of a thickness of 2-3 mm were polished to about 1 mm surface finished. The sample was clamped in a jig as featured in Fig. 3.10. The jig consists of a supporting structure and electrical connections. The supporting structure is a stainless steel skeleton covered by glass sleeving. The sample is held under pressure between high purity silica glass discs and the electrical contact to the sample is made via connections consisting of: i) gold foils in contact with both sample electrodes, ii) platinum (Pt) lead connected to the gold foil, one end of which goes to the data acquisition unit. The Pt leads have to be shielded in silica glass tubes to eliminate stray capacitance. The thermocouple is inserted close to the sample to monitor its temperature.

The dielectric response was measured using an impedance analyser (HP Model 4284A), at wide temperature range using electric tube furnace for the temperature range 25-400 ^{o}C and cryostat system for the temperature range from –50 ^{o}C to room temperature (25 ^{o}C). A frequency in a range of 1 – 100 kHz was applied. The impedance analyser was used in conjunction with a computer-controlled temperature chamber to measure capacitance as a function of frequency and temperature. The temperature was measured via a platinum resistance thermocouple mounted directly on the ground electrode of the sample fixture. A measured capacitance value was converted to dielectric constant, ε_r, using the following equation:

$$\varepsilon_r = Cd/\varepsilon_o A \qquad (3.10)$$

where C is the capacitance (F), d is the thickness (m), and A is the area (m^2) of the samples, ε_o is the permittivity of free space (8.85434 x 10^{-12} F/m).

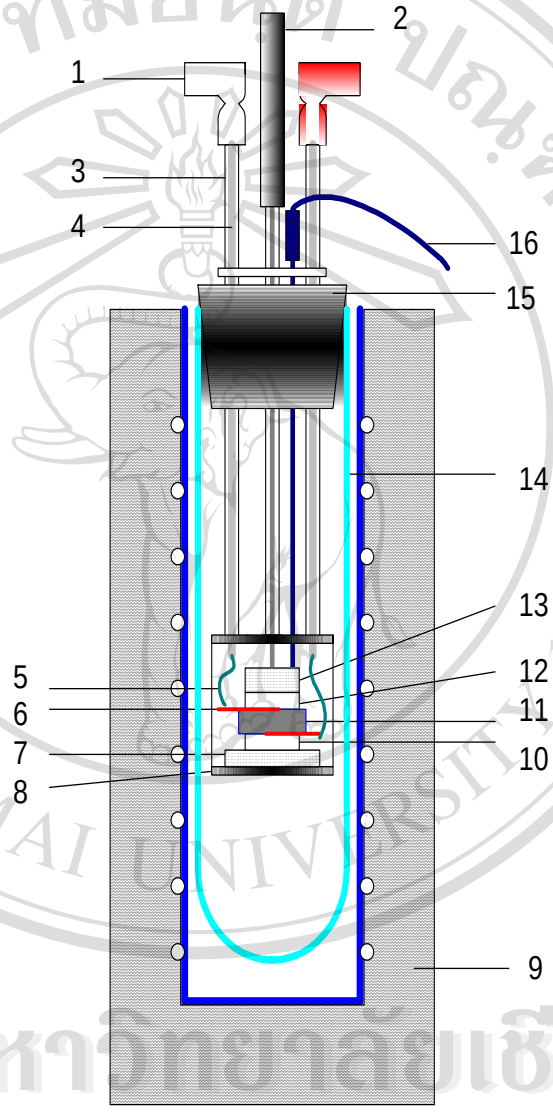

Fig. 3.10 Cross section view of the jig and details of arrangement: 1 BNC head, 2 Spring loaded plunger, 3 Stainless steel skeleton, 4 Silica glass tube fit inside stainless steel rod, 5 Pt lead, 6 gold foil, 7 & 13 ceramic discs, 8 sample support part, 9 Wound tube furnance, 10 & 12 Silica glass discs, 11 Sample disc, 14 Glass sleeve, 15 Rubber bung and 16 R-type thermocouple.